

OPTICAL TIME DOMAIN REFLECTOMETRY

OPTICAL TIME DOMAIN REFLECTOMETRY

by

RANDALL EWEN PARK

PART B: OFF-CAMPUS PROJECT

A project report submitted in partial fulfillment of  
the requirements for the degree of  
Master of Engineering

Department of Engineering Physics

McMaster University

Hamilton, Ontario, Canada

1981

MASTER OF ENGINEERING (1981)

McMASTER UNIVERSITY

Department of Engineering Physics

Hamilton, Ontario

TITLE:       Optical Time Domain Reflectometry

AUTHOR:       Randall Ewen Park, B.Sc. (Simon Fraser University)

SUPERVISOR: Dr. L.A. Godfrey


Number of Pages: vii, 48

## ABSTRACT

This report is a theoretical and experimental study of optical time domain reflectometry techniques as applied to fiber optic systems. It predicts system performance for measurements of fiber breaks and discontinuities, fiber attenuation, and fiber dispersion. Two systems are shown to be needed for the two common types of future fiber systems. For single mode fibers at 1300 nm, an ultra short ( $<100$  psec) light pulse is needed for a system which could check for breaks and measure dispersion. For graded index fibers at 900 nm, a sensitive system using a 1 nsec pulse and amplifiers could be built to measure fiber attenuation properties using Rayleigh backscattering as well as for break detection and dispersion measurements. An ultra fast light source was constructed and used in an experimental optical time domain reflectometer system which is described. Recommendations as to components to use in the system are given.

## ACKNOWLEDGEMENTS

The author would like to express his thanks to Dr. L.A. Godfrey of Opto-Electronics Ltd. for his supervision and encouragement. Thanks also to Van Tzannidakis and everyone else at Opto for helpful suggestions.



## TABLE OF CONTENTS

	<u>Page</u>
ABSTRACT	iii
ACKNOWLEDGEMENTS	iv
TABLE OF CONTENTS	v
LIST OF ILLUSTRATIONS	vii
CHAPTER 1: INTRODUCTION	1
CHAPTER 2: THEORY	9
2.1 Measurable Parameters	9
2.2 Component Parameters	11
2.2.1 Sources	11
2.2.2 Detectors	11
2.3 Power Considerations	12
2.4 Rayleigh Backscattering Amplitudes	14
2.4.1 Multimode graded index fiber	15
2.4.2 Single mode fiber	17
2.5 Dispersion Measurements	17
2.5.1 Modal Dispersion	18
2.5.2 Waveguide Dispersion	18
2.5.3 Material Dispersion	18
CHAPTER 3: OPTICAL Y COUPLERS	22
CHAPTER 4: LASER HEAD CONTROL UNIT	25
4.1 Introduction	25
4.2 Pulse Generator	25
4.3 Trigger Generator	28
4.4 Power Supplies	30
4.5 Digital Panel Meter	32
CHAPTER 5: LASER HEAD CHARACTERISTICS	34
CHAPTER 6: OTDR EXPERIMENTS	36
6.1 Optical Y Couplers	36
6.2 Experimental Setup	38
6.3 Single Mode Fibers	40
6.4 Reflection Coefficients for Non-Ideal Breaks	41

CHAPTER 7: OTDR SYSTEM RECOMMENDATIONS	43
7.1 Couplers	43
7.2 Pulse Width	43
7.3 Amplifiers	44
CHAPTER 8: CONCLUSIONS	46
REFERENCES	48

## LIST OF ILLUSTRATIONS

<u>Figure</u>		<u>Page</u>
1-1	Multimode Graded Index Fiber	2
1-2	Cladding Mode Stripper	2
1-3	Mode Mixer	4
1-4	OTDR System	4
1-5	OTDR Return Signal	7
2-1	Detector Output vs. Effective Reflection Coefficient	13
2-2	Backscattered Powers	16
2-3	Wavelength of Zero Material Dispersion vs. Concentration of Additive	20
2-4	Fiber Transit Time vs. Wavelength	20
2-5	Material Dispersion vs. Wavelength	20
3-1	Four Port Coupler	23
3-2	Selfoc Coupler	23
3-3	Selfoc Coupler	23
3-4	Evanescent Coupler	23
3-5	Biconical Taper Coupler	23
4-1	Control Unit	26
4-2	Pulse Generator	27
4-3	Trigger Generator	29
4-4	Power Supplies	31
4-5	Digital Panel Meter	33
5-1	Laser Head Spectra	35
6-1	Maximum Coupling Efficiency	37
6-2	Measuring Coupling Efficiency	37
6-3	Experimental OTDR Setup	39
6-4	Reflection Coefficient Measurements	39



## 1 INTRODUCTION

Optical fiber transmission systems are emerging as viable high speed, long distance communication links. They have a number of important advantages over traditional wire or coaxial cable systems such as higher bandwidth, longer distances between repeaters, smaller size, and immunity from electrical and magnetic interference. The main disadvantage of fiber systems is cost, but increased production volume is bringing component and fiber costs down.

In the optical fiber systems, a light signal carries the information along an optical fiber light guide. A typical system uses a pulsed laser diode as the source, a multimode graded index fiber as the light guide, and an avalanche photodiode as the detector.

The various types of modes in a graded index fiber are shown in figure 1-1. The parabolic profile of the core index of refraction guides the various modes down the fiber in sinusoidal paths. Although the higher order modes travel a longer distance in the core, most of this distance is in the lower index glass near the edges where the light travels faster. Thus the propagation time is (theoretically) the same for all the modes and the modal dispersion (pulse broadening due to the different propagation times of the modes) is very small. The exceptions are the cladding modes (fig 1-1) which are modes which are launched at an angle greater than the core acceptance angle. These modes can still propagate because of total internal reflection at the cladding-air or

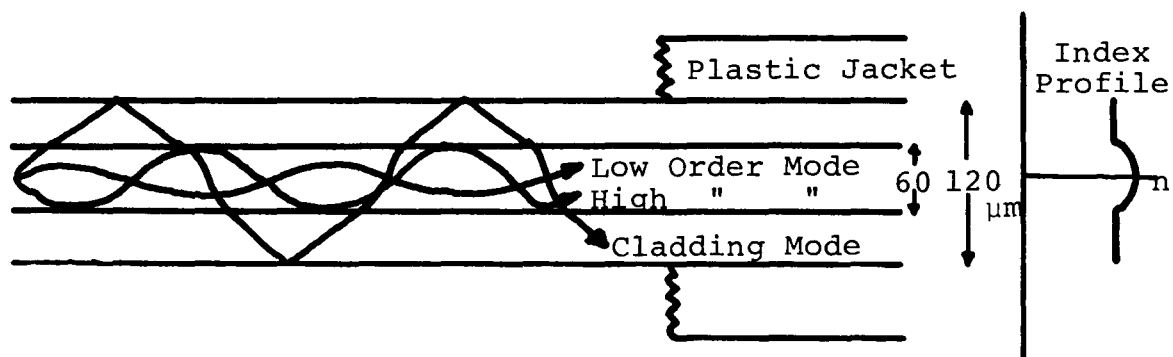


FIGURE 1-1 MULTIMODE GRADED INDEX FIBER

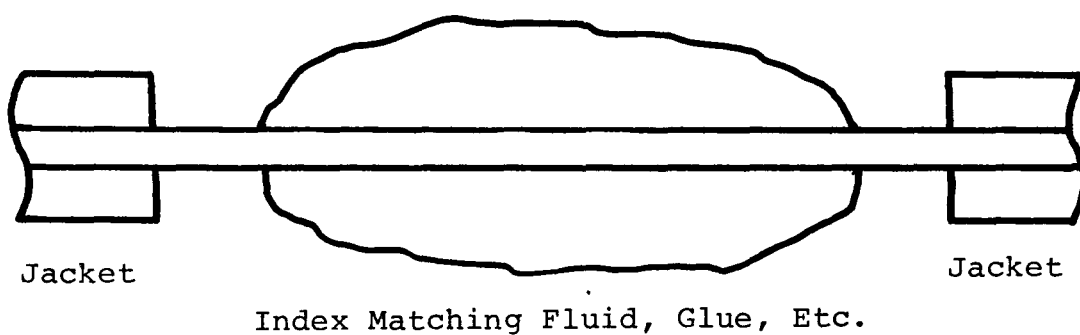


FIGURE 1-2 CLADDING MODE STRIPPER

cladding-jacket interface. Since they travel a much longer path than the core modes, they greatly increase pulse dispersion. The cladding modes can be attenuated somewhat by making the plastic jacket of a fairly high index of refraction, lossy material. A cladding mode stripper (fig 1-2) can also be used. The cladding modes are coupled out of the fiber by the index matching material and are radiated by it.

Coupling of light from one core mode to another occurs in all fibers because of imperfections along the fiber axis. Until the steady state mode coupling situation is reached, when the energy leaving a particular mode is equal to the energy mixed into that mode, the measured attenuation coefficient per unit length will not be constant. This steady state mode coupling length of the fiber ranges from tens to thousands of meters. A mode mixer can be constructed by repeatedly bending the fiber (fig 1-3) to deliberately couple the modes and help produce the steady state situation.

A major consideration in fiber systems is the coupling from source to fiber and fiber to detector. Virtually all photo detectors used have active areas and acceptance angles which are larger than the fiber cores and radiation angles. Thus the fiber-detector coupling efficiency approaches 100%. The source-detector coupling, however, is not usually as good. Most of the multi-heterostructure diode lasers used for optical communications have large emitting angles and small areas. If the emission angle is larger than the core acceptance angle, the undesirable cladding modes will be excited and a mode stripper may be necessary. The small, rectangular emitting area of the laser will

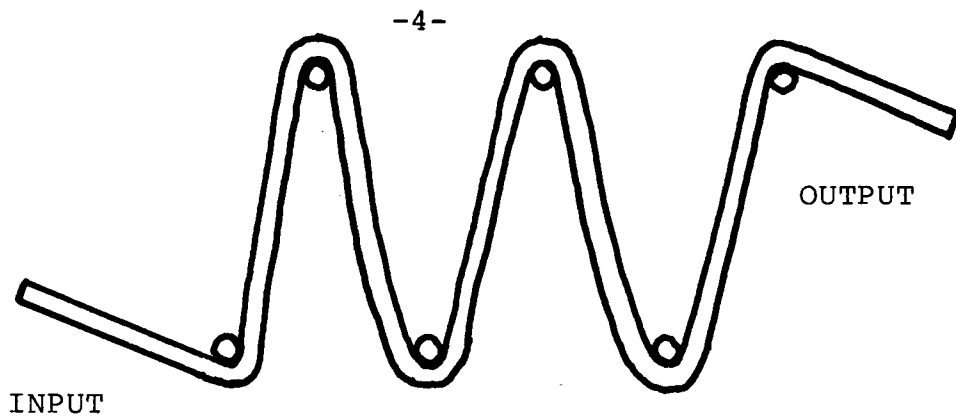


FIGURE 1-3 MODE MIXER

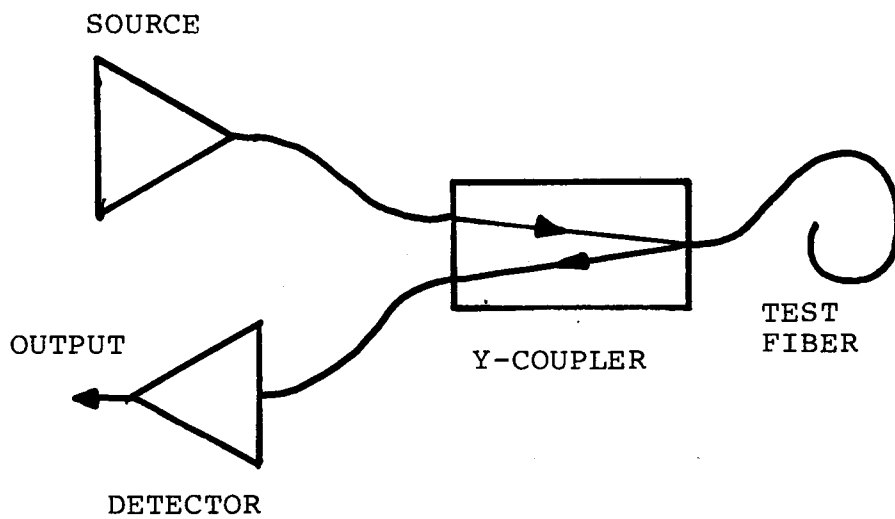


FIGURE 1-4 OTDR SYSTEM

not produce steady state excitation of the core modes, and a mode mixer will be necessary.

In optical fiber transmission systems, splices and connectors are also needed. A typical link may have five one kilometer lengths of fiber spliced together. There is also the possibility of fiber breakage during installation. A measurement system is necessary to pinpoint faulty splices, fiber breaks, and areas of high loss. Fiber dispersion measurements are also needed, both for new fibers and installed systems. System loss measurements can be made in the transmission mode, but the measured loss is a function of many variables, including splice and coupler loss, break loss, fiber attenuation and dispersion, and mode coupling losses. In particular, fiber splices and couplers usually have some variation in their performance. The source and detector alignment is critical in achieving reproducible loss measurements. The two point method of measuring attenuation of the fiber and then cutting off a section and remeasuring gives the attenuation of the cut off section. This relaxes the source coupling conditions, but only gives the attenuation for a short section, and the discarded one at that. The possibility of non-uniform fiber attenuation means that a faulty short length of fiber could introduce uncharacteristically high losses. Fiber breaks can introduce losses in magnitude from approximately 0 to 100%, and the transmission method can not pinpoint the break position. Finally, if the fiber is shorter than the steady state coupling length, the attenuation coefficient will not have reached constant value. Destructive testing is the only way to determine the steady state

coupling length with the transmission system of measurement.

Time domain reflectometry is an established test method in microwave circuitry. It is used to find discontinuities in transmission lines, check impedance, and can be used to estimate bandwidth. In microwave time domain reflectometry, a fast (25 psec rise time) step function or delta function is injected into the test line, and the electrical reflection is observed. A similar setup can be used for testing optical fibers (fig. 1-4). As with the microwave time domain reflectometer, the optical time domain reflectometer (OTDR) can measure the positions and magnitudes of discontinuities<sup>1</sup>. By observing the Rayleigh backscattering amplitude, the attenuation of the fiber can also be determined<sup>2,3</sup>, and the change in attenuation with position can give the steady state coupling length (fig. 1-5).

There were two main aims to this project. The first was to construct an ultrashort pulsed laser diode source and control unit and characterize the source. The second was to use this source and a fast detector to set up an experimental OTDR system and do a feasibility study on the system.

Chapter 2 covers calculations for the OTDR system such as pulse width, system range, etc. Chapter 3 discusses various types of fiber Y-couplers and describes construction of fused biconical taper couplers. Chapter 4 gives details of a control unit constructed to be used with an Opto-Electronics laser head to produce short light pulses for use with the OTDR. Chapter 5 gives some characteristics of the assembled source. Chapter 6 describes the experiments done in connection with the OTDR.

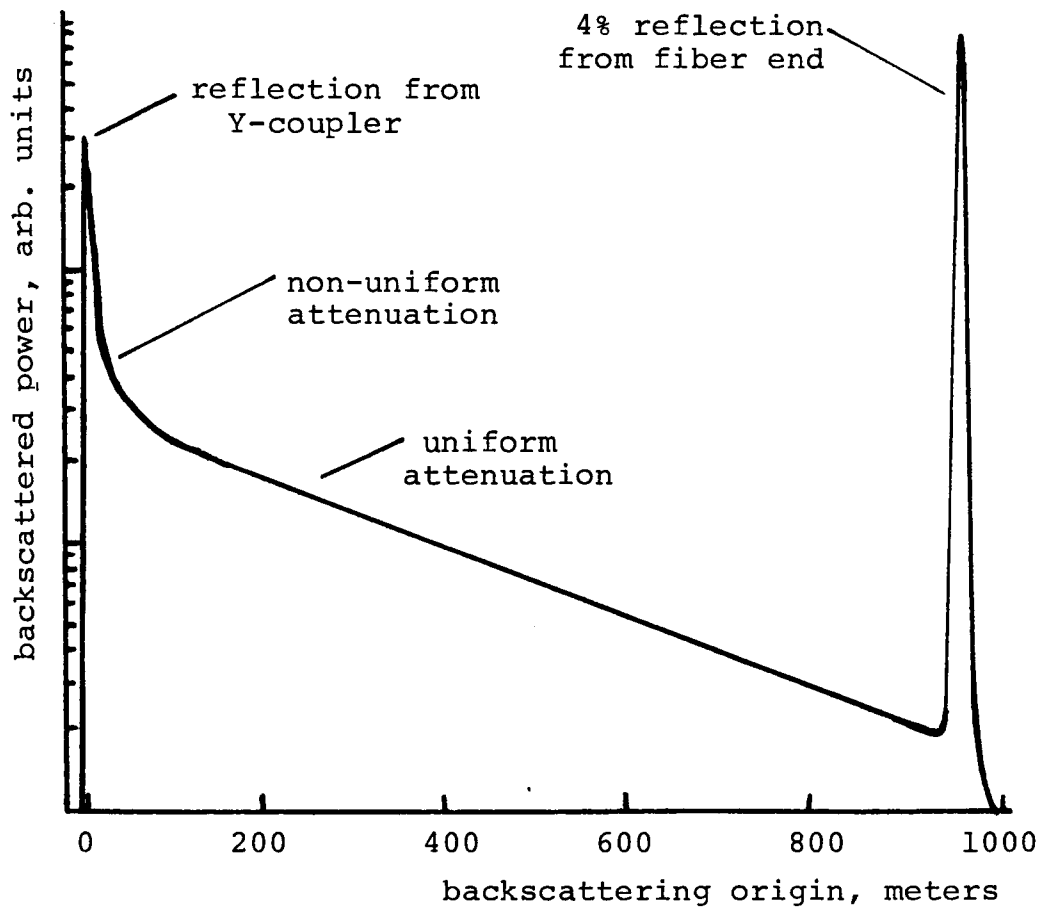


FIGURE 1-5 TYPICAL OTDR RETURN SIGNAL

Chapter 7 recommends improvements to the system, and Chapter 8 gives conclusions.



## 2 THEORY

### 2.1 Measurable Parameters

The fiber parameters which can be measured by both the reflection and transmission methods are listed in table 1 (Y=yes, P=possible, N=No).

TABLE 1

<u>PARAMETER</u>	<u>MEASUREMENTS &amp; METHODS</u>	
	<u>TRANSMISSION</u>	<u>METHOD</u> <u>REFLECTION</u>
<u>Discontinuity Amplitude</u>	P	Y
<u>Discontinuity Position</u>	N	Y

Note: amplitude can be estimated by decrease in transmission above normal attenuation, but reflection would be better

<u>Dispersion (Modal)</u>	Y	Y
---------------------------	---	---

Note: dispersion can be measured using reflection setup; advantage is twice the dispersion for the same fibre length

<u>Dispersion (Spectral)</u>	Y	Y
------------------------------	---	---

Note: same method as modal dispersion, but a broader (LED) source may be necessary

<u>Fibre Attenuation</u>	P	Y
--------------------------	---	---

Note: for transmission, must allow for coupling, etc. losses; for reflection, must measure Rayleigh scattering amplitude

<u>Steady State Mode Position</u> <u>(Non-destructively)</u>	N	Y
---	---	---

<u>Propagation Losses (Total)</u>	Y	Y
-----------------------------------	---	---

Note: can be measured in reflection by observing 4% reflection after round trip

Discontinuities may be due to splices, connectors, breaks, or even small radius bends. Modal dispersion was discussed in the introduction. Spectral dispersion is pulse broadening due to the finite spectral width of the source and the dependence of velocity on wavelength in the glass. Fiber attenuation is the loss solely due to the fiber properties. The steady state mode position was discussed in the introduction. Total propagation loss is the actual attenuation of the whole link, including all the above. As can be seen, the reflection method can measure all the parameters that the transmission method can, some in a much simpler manner.

Table 2 shows the approximate detection speeds needed for measuring the various parameters in the reflection mode.

TABLE 2

<u>Parameter</u>	<u>Minimum Detection Speed</u>	<u>Notes</u>
Discontinuity amplitude	S	Accuracy 3m-1m
Discontinuity position	S-M	
*Dispersion	F	
Propagation Losses (Total)	S	
Steady State mode Position	S	
Fiber attenuation	S	

\*1-2nsec for typical 1 km graded index multimode fiber at 900 nm.

S - slow      < 40 MHz  
                 ~

M - medium    ~ 100 MHz

F - fast       > 500 MHz  
                 ~

For dispersion measurements, a fast oscilloscope and detection

system is needed, since for a 1 km multimode fiber at 900nm the total dispersion is approximately 1-2nsec and is smaller for single mode fibers or 1300nm wavelength. In this case, though, signal level is not a problem since a 100% mirror can be butted to the far end of the test fiber for the reflection setup, giving a large return (and twice the propagation distance of the transmission method). If only the position of discontinuities needs to be known to ~1m, a moderately fast (100 MHz) detection system is all that is needed for attenuation and discontinuity measurements.

## 2.2 Component Parameters

### 2.2.1 Sources

The sources used for the experiments were pulsed laser diodes.

Source parameters were:

Peak Power	2W
Repetition rate	100Hz - 20kHz
Pulse Width	70psec - 1nsec
Wavelength	900nm
Spectral Width	2.4nm
Emitting Area	2 x 76 $\mu$ m
Beam Divergence (FWHM)	7 <sup>o</sup> x 10 <sup>o</sup>

### 2.2.2 Detectors

Available Si detector parameters were as follows:

<u>Type</u>	<u>Sensitivity</u>	<u>Gain</u>	<u>FWHM for 70psec Optical Pulse</u>
Non-avalanching	0.2 A/W	-	100psec
Avalanching	0.2 A/W	50	140psec

Avalanching                      0.2 A/W                      200                      300psec

### 2.3 Power Considerations

The range of the OTDR system will be limited by the received signal amplitude. The power reaching the detector on return will be

$$P_d = P_o T_\ell T_d r 10^{-\alpha 2L/10} \quad (1)$$

where  $P_o$  = laser power,  $T_\ell$  = effective laser coupling into fiber,  $T_d$  = fiber coupling into detector,  $r$  is effective reflection coefficient from discontinuity,  $\alpha$  is attenuation coefficient in dB/km,  $L$  is length in km.

The detected signal voltage will be

$$V_d = i_d R D = S G P_d R_L D \quad (2)$$

where  $S$  is detector sensitivity,  $G$  = avalanche gain,  $R_L$  is load resistor, and  $D$  is a factor which allows for the decrease in pulse height due to dispersion.

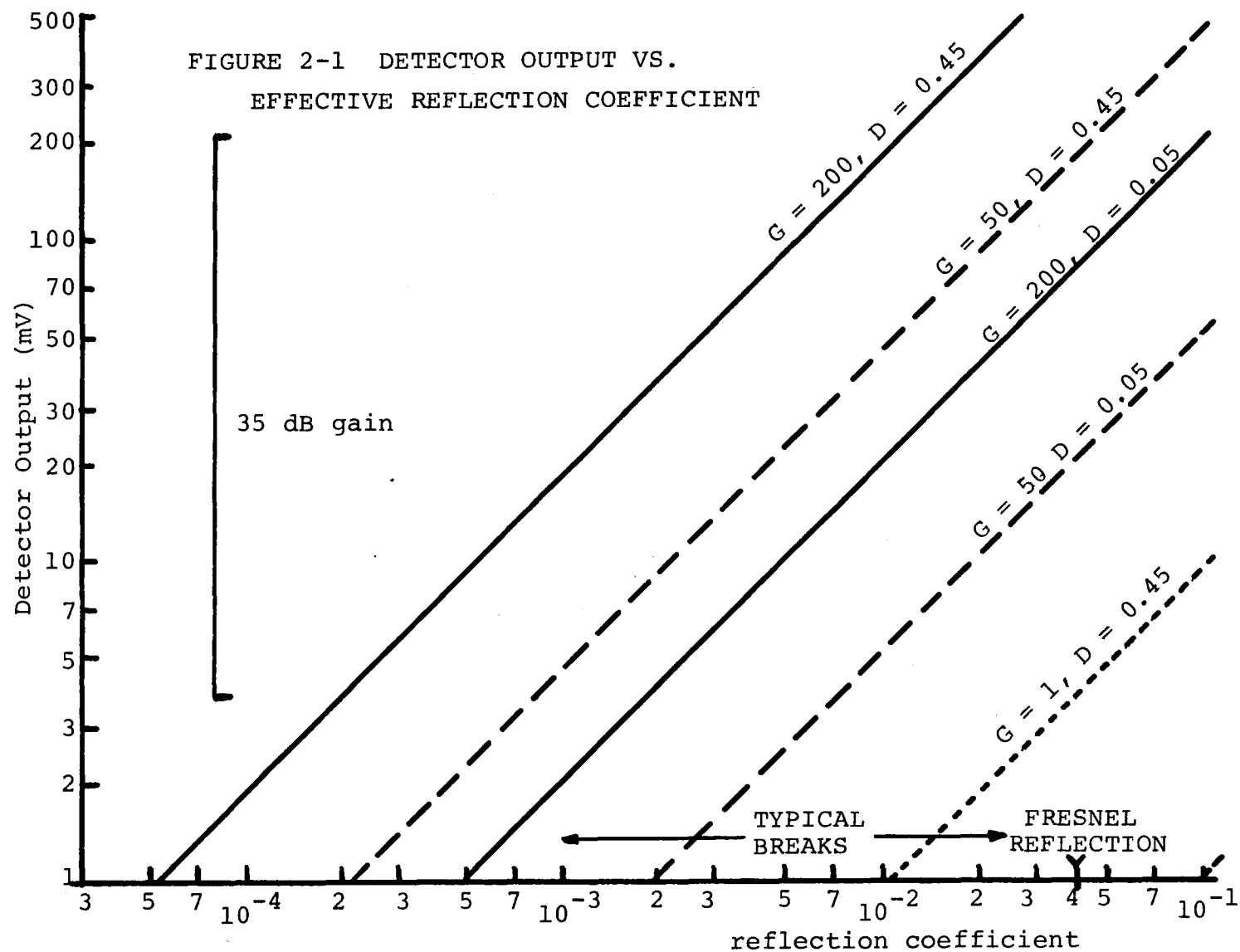
Combining (1) and (2),

$$V_d = S G R_L P_o T_\ell T_d r 10^{-\alpha 2L/10} D \quad (3)$$

Taking typical parameters for source, coupling, and detector:  $P_o = 2W$ ,  $T_\ell = 30\%$  (40% at Y-coupler, 75% into fiber),  $T_d = 35\%$ ,  $\alpha = 5$ , 10dB/km,  $L = 2km$ ,  $S = 0.2$  A/W (for all detectors considered),  $R_L = 50 \Omega$ , gives

$$\begin{aligned} V_d &= 0.21 GrD \text{ volts (5dB/km)} \\ V_d &= 0.021 GrD \text{ volts (10dB/km)} \end{aligned} \quad (4)$$

Taking a minimum detection level of  $\sim 1mV$  for direct connection to an oscilloscope, the detector output can be plotted (fig. 2-1). For a 1km, 500MHz fiber, the round trip dispersion is 2nsec. Thus  $D$  for a



100psec pulse is 0.05 and for a 1nsec pulse is 0.45, assuming Gaussian pulse widths which add as the sum of squares. Note that for increased detection sensitivity at the expense of detection speed, a larger load resistor can be used.

## 2.4 Rayleigh Backscattering Amplitudes

To determine the attenuation of an optical fiber with the OTDR, the Rayleigh backscattered power is observed. Neumann<sup>4</sup> gives the ratio of the power Fresnel reflected from the cleaved end to the backscattered power as

$$\frac{P_r}{P_s} = \frac{2R}{\alpha_s v_g t S} \quad (5)$$

where R equals 0.04 for the 4% reflection,  $\alpha_s$  is the Rayleigh scattering loss per unit length,  $v_g$  is the group velocity, t is the pulse width, and S is the fraction of scattered light which is returned down the fiber. Personick<sup>2</sup> gives this fraction as

$$S = \frac{(NA)^2}{4n^2} \quad (6)$$

for isotropic scattering, with NA being the fiber numerical aperture and n being the core index of refraction. Rayleigh scattering is not isotropic however, and Neumann<sup>4</sup> calculated S to be larger by 3/2 when this is taken into account. Thus the complete expression is

$$\frac{P_r}{P_s} = \frac{16Rn^2}{3\alpha_s v_g t (NA)^2} \quad (7)$$

Note that Rayleigh scattering loss is not the only loss mechanism

in the fiber, and thus  $\alpha_s$  will be somewhat less than the total attenuation coefficient. However, the ratio between two points on the return signal will give the total attenuation over the round trip length. This can be seen by looking at fig 2-2. The fiber has a total attenuation fraction of  $\beta$  in distance  $x_0$ . Then for an input power of  $P_0$  at  $x=0$ , the transmitted power at  $x_0$  will be  $\beta P_0$ . If the fractional scattering constant is  $\alpha$ , then the scattered powers at  $x=0$  and  $x=x_0$  are  $\alpha P_0$  and  $\alpha \beta P_0$  respectively. Thus the received backscattered power at  $x=0$  is  $\alpha P_0$  from the scattering at  $x=0$  and  $\alpha \beta^2 P_0$  from the scattering at  $x=x_0$ . The ratio of these two is

$$\frac{\alpha \beta^2 P_0}{\alpha P_0} = \beta^2 \quad (8)$$

which is the attenuation fraction for the length  $2x_0$ . Note that this discussion has considered scattered power, and that dispersion of the pulse would reduce the backscattered signal amplitude. If the dispersion of the fiber is measured, the signal amplitude can be multiplied by a correction factor.

#### Numerical Examples:

##### 2.4.1 Multimode graded index fiber

Converting a typical Rayleigh scattering loss of the fiber, 2 dB/km, to nepers/meter ( $1 \text{ neper/m} = 4.33 \times 10^3 \text{ dB/km}$ ),  $\alpha_s = 4.6 \times 10^{-4}$  neper/m. Taking a typical numerical aperture of 0.2, a 1 nsec pulse,  $v_g = 2 \times 10^8 \text{ m/sec}$ , and  $n=1.5$  gives  $P_r/P_s = 51 \text{ dB}$ . A 10 nsec pulse would increase the backscattered power by 10 dB to 41 dB below the 4% reflection. Figure 2-1 shows that both these signal levels would be

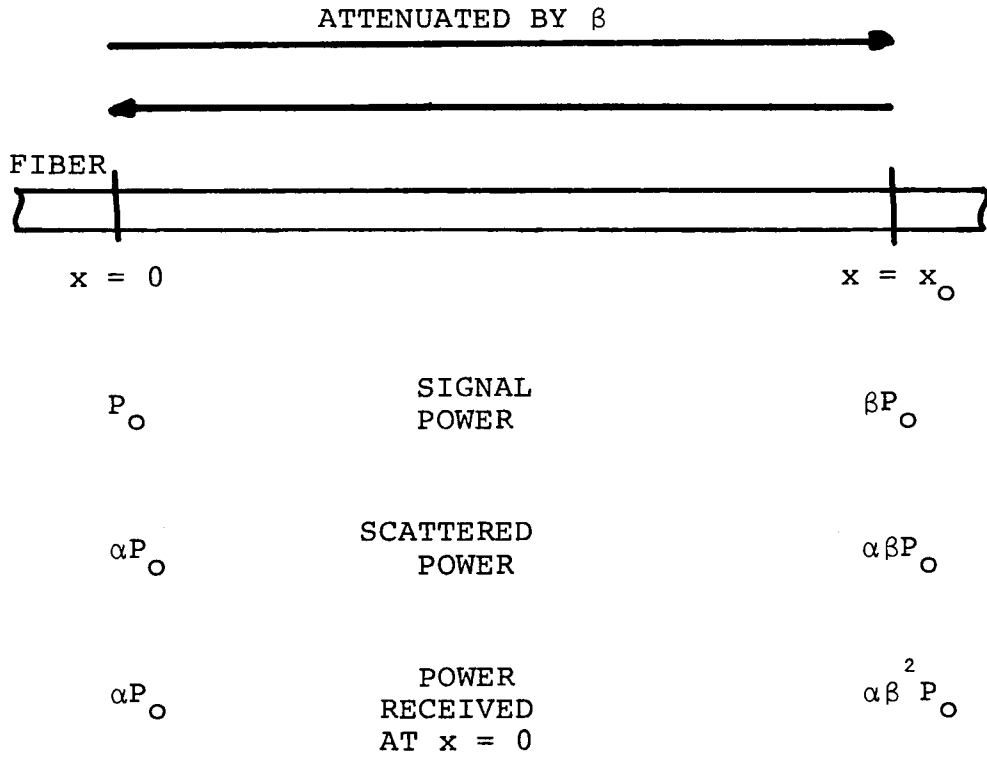


FIGURE 2-2 BACKSCATTERED POWERS



measurable with the avalanche detector with  $G = 200$ .

#### 2.4.2 Single Mode Fiber

For single mode fibers at 1300 nm, the loss due to Rayleigh scattering is smaller, approximately 0.5 dB/km or  $1.2 \times 10^{-4}$  neper/m. Using  $NA = 0.2$ ,  $n = 1.5$ ,  $v_g = 2 \times 10^8$  and a 70 psec pulse gives  $P_r/P_s = 69$  dB, while a 10 nsec pulse gives  $P_r/P_s = 47$  dB. Fig 2-1 shows that the 10 nsec pulse would give a detectible signal, but the 70 psec pulse would not.

#### 2.5 Dispersion Measurements (transmission mode or reflection mode with $r=1$ at far fiber end)

The pulsed laser-silicon detector (non-avalanching) system which was operational at 0.9  $\mu\text{m}$  had a combined FWHM of 100 psec at a signal level of 1V. Assuming Gaussian pulse shapes, this system could measure a pulse broadening as small as  $80 \text{ psec} \pm 3 \text{ psec}$  or  $100 \text{ psec} \pm 2 \text{ psec}$ . For a reasonably large detected signal (say  $\sim 4\text{mV}$ ) one could stand 250 X attenuation or 24dB. Assuming a combined loss of 9dB for source and detector coupling, a loss of  $\sim 15\text{dB}$  could be tolerated in the fiber. For a high performance fiber,  $\sim 3\text{dB/km}$  attenuation, lengths up to 5km could be tested. For a measurable dispersion of  $\tau = 100 \text{ psec}$ , the equivalent 3dB bandwidth is given by

$$B_{3\text{dB}} = \frac{0.44 \text{ GHz}}{\tau \text{ (nsec)}} \quad (9)$$

or

$$B_{3\text{dB}} = 4.4 \text{ GHz}$$

Over a 5 km length, a fiber with a bandwidth product as high as  $\sim 22\text{GHz-km}$  could be tested.

Typical dispersion measurements;

#### 2.5.1 Modal dispersion (multimode graded index fibers)

The theoretical minimum for the dispersion of a perfect graded index fiber is  $\sim 7 \text{ psec/km}^5$ . In practice due to the difficulty in fabricating perfect profiles, the best experimental values are at least 20 times this, or  $150 \text{ psec/km}$ . Thus the minimum traversed length of fiber for this measurement using the fastest detector - source would be  $0.75 \text{ km}$  to give an easily measurable  $100 \text{ psec}$  broadening. Common graded index fibers have bandwidth of  $300\text{--}500 \text{ MHz/km}$  giving dispersion values of  $1\text{--}3 \text{ nsec/km}$ ; thus dispersion could be measured with  $100 \text{ m}$  of fiber.

#### 2.5.2 Waveguide dispersion (single mode fiber)

The carrying capacity of a single mode fiber may be ultimately limited by waveguide dispersion caused by the frequency dependence of the group velocity of a mode. The fundamental limit at the point of zero material dispersion depends on the source spectral bandwidth squared and is approximately  $10^{-2} \text{ psec/km-nm}^2$ . This will be much below the limits of measurement of this system. In practice, this system would be able to put a lower limit on the bandwidth of the fiber of, as stated earlier,  $\sim 22 \text{ GHz-km}$  (or higher if the fiber has less than  $3 \text{ dB/km}$  attenuation, allowing a longer test length). Also, waveguide dispersion in a single mode fiber at wavelengths away from the optimum can approach  $6 \text{ psec/km-nm}$ , which (for  $2.4 \text{ nm}$  spectral width) would be measurable for  $\sim 5 \text{ km}$  of fiber.

#### 2.5.3 Material dispersion

a)  $900 \text{ nm}$  At  $900 \text{ nm}$ , typical fiber dispersion is  $\sim 70 \text{ psec/km-nm}^5$

For this source, the material dispersion would be  $\sim 175 \text{ psec/km}$ . This amount in theory would be measurable over a distance of  $\sim 0.5 \text{ km}$ , but in practice would be masked by modal dispersion for typical fibers, unless a larger spectral width source was used.

b) 1300nm In this region, fiber dispersion approaches zero for certain wavelengths. However, dispersion can be determined from the variation of the optical transit time with wavelength.

The main difficulty in characterizing this material dispersion with a pulsed laser diode is that this wavelength of zero dispersion is strongly dependent on the fiber composition (fig. 2-3)<sup>7</sup>. The common method of determining the fiber dispersion in this region is to measure the transit time of a pulse in the fiber over a range of wavelengths straddling the zero (fig. 2-4)<sup>7</sup>. From this plot, it is clear that a wavelength range of at least  $\pm 100 \text{ nm}$  about the zero (which itself can vary over  $\sim 100 \text{ nm}$ ) is needed for a reasonable measurement. The most which could be expected from temperature tuning the laser diode with a thermo-electric cooler would be  $\pm 10 \text{ nm}$ . Thus this technique could not be used with this system. Dispersion could be measured directly, and the 22 GHz-km measurement limit applied to the fiber if the dispersion of the fiber at the laser wavelength was less than the minimum measurable  $\sim 5 \text{ psec/km-nm}$ . The choice of the laser wavelength would be important because of the dependence of dispersion on wavelength. Figure 2-5<sup>7</sup> shows dispersion vs. wavelength for typical optical fibers.

#### c) Broader Sources

An alternative approach which might be considered for material

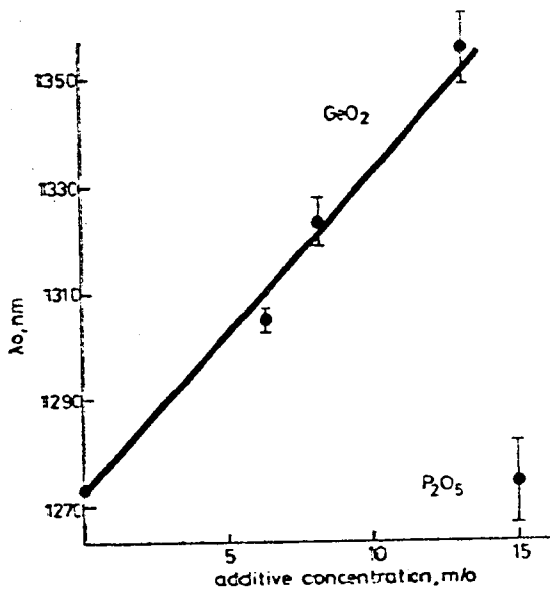


FIGURE 2-3  
(ref. 7)

*Effect of concentration of additive on wavelength  $\lambda_0$  of zero of material dispersion*

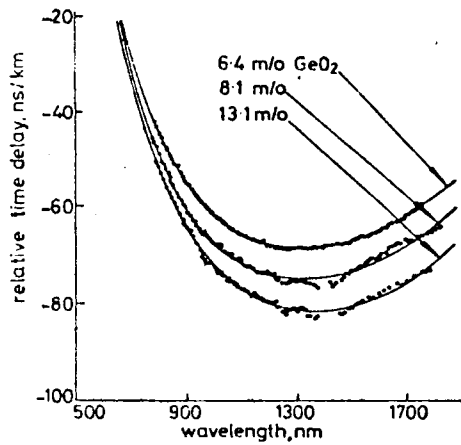


FIGURE 2-4  
(ref. 7)

*Fibre transit time per kilometre relative to that at 580 nm*

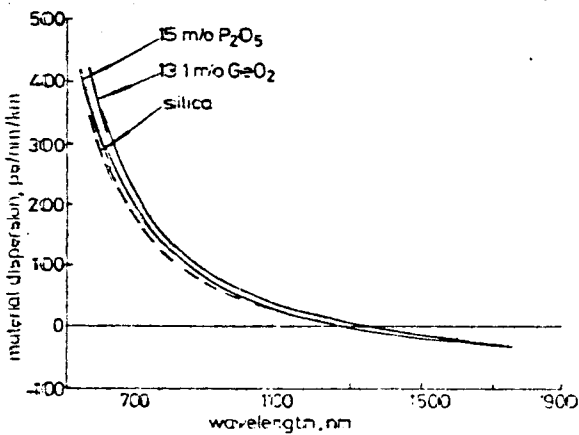


FIGURE 2-5  
(ref. 7)

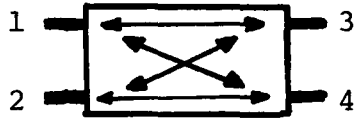
*Comparison of material dispersion of fibres*

dispersion measurements at both 900 and 1300nm is to use an LED for the source. Typical LED's have spectral widths of 25-40nm at 900nm wavelength, and 50-100nm at 1300nm wavelength. In this case, material dispersion at 900nm would be  $\sim 2\text{nsec/km}$  which should enable dispersion measurement. At 1300nm, dispersion data from an LED whose spectrum straddled the dispersion zero would be difficult to interpret without being able to change the wavelength, and away from the dispersion zero, the laser system can measure to  $\sim 5\text{psec/km/nm}$ , so there is no advantage in using the LED.

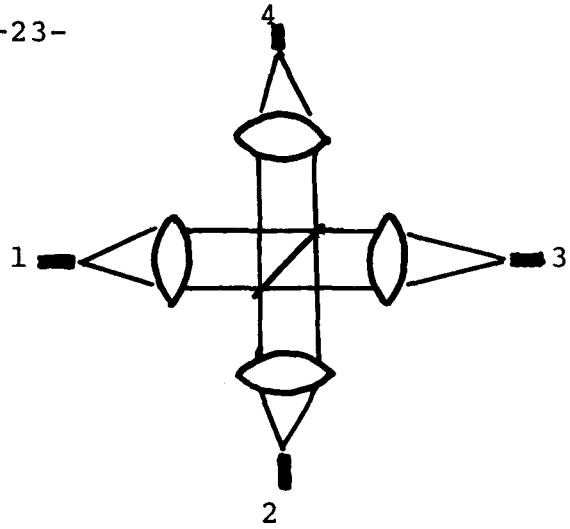
### 3. OPTICAL Y COUPLERS

For optical time domain reflectometry, the source injects a pulse of light into the test fiber and the detector detects the reflected signal from discontinuities. Thus the source and detector have to couple into and out of one end of the optical fiber. The Y coupler needed here is basically a four port coupler with one port unused (fig. 3-1). There are two basic types of fiber Y couplers. The first type does not make use of the waveguiding properties of the fiber, while the second type does make use of these properties to do the coupling.

In the first group are discrete lens-beam splitter arrangements as well as Selfoc types. The disadvantages of a discrete lens system are clear: coupling problems, optical alignment, bulk, and cost. The main advantages of the Selfoc types are that they are compact and that the faces of the components can be cemented together after alignment. Fig. 3-2 shows a Selfoc equivalent of a standard lens-beam splitter arrangement<sup>8</sup>. For an OTDR system, one lens and fiber would be omitted. The 45° angle of the beam splitter means that this device is polarization sensitive, which may or may not cause problems depending on the actual layout. Commercial couplers of this design have typical insertion losses of 1.5 dB. A simpler Selfoc coupler is shown in fig. 3-3<sup>9</sup>. This one uses the property of 1/4 pitch Selfoc lenses that off axis point sources form parallel beams. The beam splitter reflects some of this beam back to an adjacent fiber, and transmits some to an



(a)



(b)

Figure 3-1 Four Port Coupler (a) schematic (b) practical

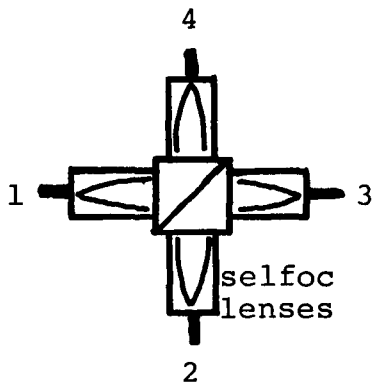


Figure 3-2 Selfoc Coupler

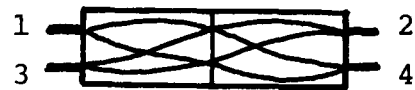


Figure 3-3 Selfoc Coupler

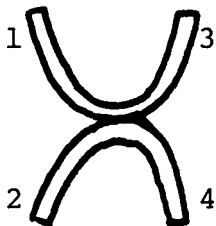


Figure 3-4 Evanescent Coupler



Figure 3-5 Taper Coupler

opposite fiber. Here again only three fibers are necessary. Insertion losses of 1.2 dB have been obtained.

The second type of coupler includes evanescent couplers and tapered biconical. The evanescent coupler has two adjacent fibers which are bent to cause radiation from one into the other (fig 3-4). Only a small amount of experimental work was done on this type because of the low coupling ratio.

The tapered biconical coupler (fig 3-5) consists of two fibers which are twisted together, tapered over this twist, and fused where they contact. The principle of operation is that light travelling down the input fiber core is converted into cladding modes by the taper. The light is still confined by the index difference between the cladding and air, but where the two fibers touch there is no index difference and the light is coupled into the other fiber. Duck<sup>9</sup> reports a typical excess loss from a biconical taper coupler of 2 dB.



## 4. LASER HEAD CONTROL UNIT

### 4.1 Introduction

In order to have a completely self contained pulsed laser diode source, a control unit was designed and built to drive the Opto-Electronics Ltd. prototype laser diode head. The control unit consisted of a trigger pulse generator with variable repetition rate, a passive 70 nsec delay line for use with a sampling oscilloscope, and a variable 50-400v power supply with digital meter. Fig 4-1 shows a block diagram of the control unit.

### 4.2 Pulse Generator

The requirement for the pulse generator section of the control unit was to provide a variable repetition rate (0-20kHz) trigger pulse for the trigger avalanche transistor. The output pulse had to have a fairly fast rise time (under 50 nsec) to provide reliable avalanche triggering and be on the order of a few  $\mu$ sec long maximum. The pulse to pulse jitter is not critical here since the oscilloscope pre-trigger takeoff comes after this section, but the frequency should be stable and it was required that the rep rate be readable from a ten turn dial on the front panel.

To accomplish the goal of linear frequency vs. resistance an LM331 voltage to frequency converter was used with a voltage divider. (fig. 4-2). The resistive divider was formed by  $P_1$ ,  $P_2$  and  $P_3$  with  $P_2$  being the front panel control and  $P_1$  and  $P_3$  being trimmer pots to

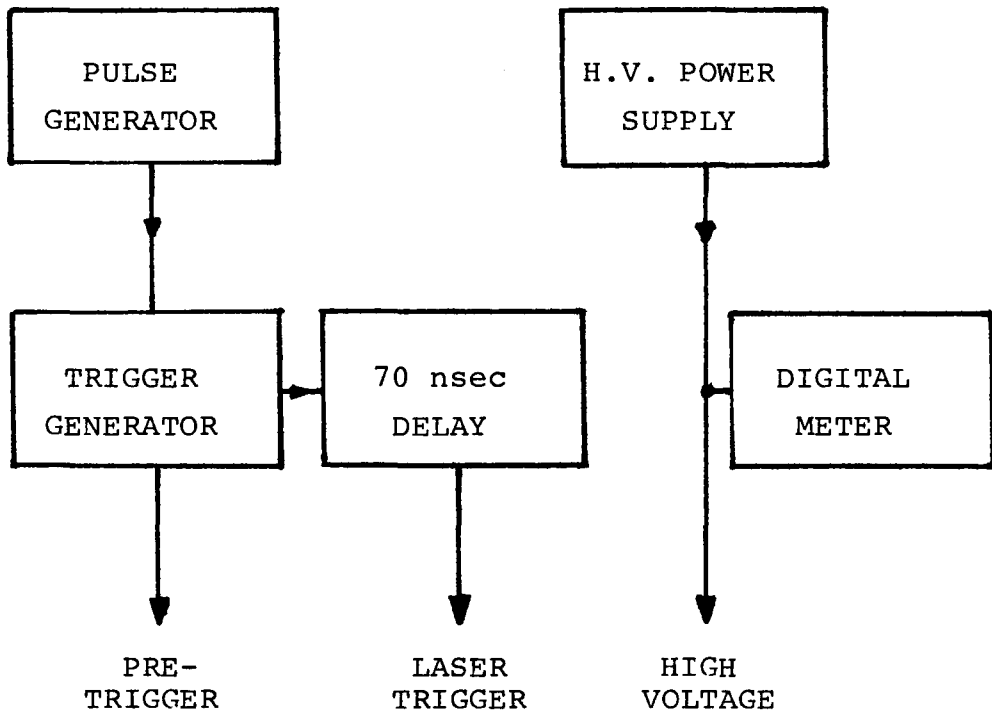


FIGURE 4-1 LASER HEAD CONTROL UNIT

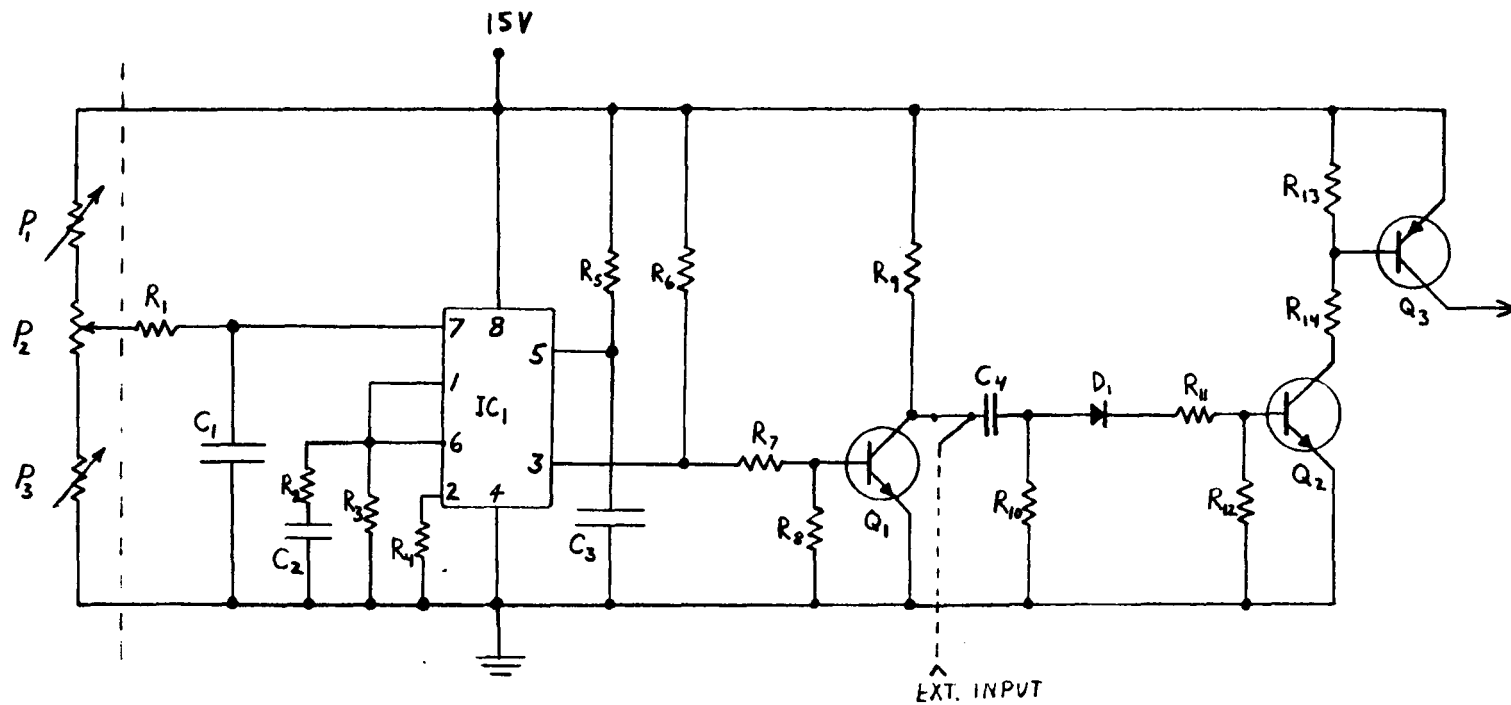


FIGURE 4-2 PULSE GENERATOR

produce the required voltage. The frequency output of this circuit is linear with voltage from a few hertz up to approximately 22kHz. With the ten turn pot and dial calibrated for 20 kHz full scale, the linearity from 100 Hz to 20 kHz is  $\pm 0.1\%$ , which is better than the pot rating of  $\pm 0.25\%$ . The dial reading from 0-10 must be multiplied by two to get the rep rate in kilohertz.

$R_7$ ,  $R_8$ ,  $R_9$  and  $Q_1$  square up the output of the voltage to frequency converter and apply it to the differentiator composed of  $C_4$  and  $R_{10}$ . The input of the differentiator has provision for an external trigger input; it will accept any positive trigger pulse greater than 200 nsec and 5V with a risetime of less than 2  $\mu$ sec and still deliver an output pulse from  $Q_3$  of less than 50 nsec risetime.  $D_1$  passes only the positive spike from the differentiator, and  $Q_2$  and  $Q_3$  switch to produce typical output pulses of 15 nsec risetime, 2  $\mu$ sec duration, and 14V amplitude.

#### 4.3 Trigger Generator

To trigger the laser head and produce a low jitter display on the sampling oscilloscope, it was necessary to have a very fast risetime trigger pulse. For this reason, it was decided to use an avalanche transistor to generate the trigger pulse (fig. 4.3). To produce the necessary pre-trigger pulse for the sampling oscilloscope, 70 nsec before the laser head trigger pulse, the laser trigger pulse was delayed by a length of RG174u coaxial cable. The  $R_4 - R_7$  network taps off a 600mV signal for the oscilloscope trigger which had a rise-time of 350 psec, FWHM of 1.5nsec. The laser trigger pulse was 10V peak with the

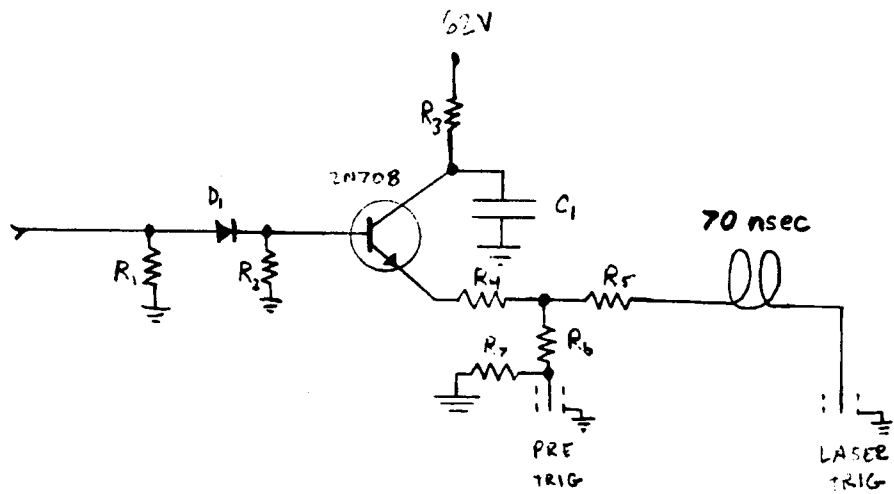


FIGURE 4-3 TRIGGER GENERATOR

cable dispersion slowing it to 700psec risetime, FWHM 3.4nsec. The fast risetime pulses, along with the use of the passive delay, resulted in display jitter of less than 5psec.

The theoretical value of  $R_4$  is equal to  $R_5$  for 50 $\Omega$  input and output, but since the transistor emitter appears as less than 50 $\Omega$ , it was found that  $R_4 = 30\ \Omega$  gave a better match. The  $R_1 - D_1 - R_2$  network was a standard base coupling circuit. The entire circuit was done on 50  $\Omega$  microstrip line with the exception of  $R_3$ , which was connected via a high impedance line to minimize high speed coupling with the supply. The original version had a higher voltage transistor (2N3019) and a diode clipper to enable adjustment of the pulse amplitude, but the faster risetime of the 2N708 was preferred over the higher voltage of the 2N3019. The diode clipper also produced reflections along the line.

#### 4.4 Power Supplies

To provide a charging voltage for the laser head discharge capacitor, a high voltage power supply was necessary. Since different laser head configurations were tried, it was necessary that this supply be variable over the range of at least 50 - 300 volts. The final configuration, which had two ranges, 50 - 200 and 100 - 400 volts, is shown in fig. 4.4. Conventional full wave centre tapped rectification was employed, and the  $R_2 - D_2$  network forms a 62V zener regulator for the trigger avalanche transistor. The high voltage regulation is controlled by floating regulator IC1, which controls the gain of series pass transistor  $Q_1$ .  $R_1$  is the short circuit sense resistor, which is set at 15mA because of secondary breakdown limitations of  $Q_1$ .  $R_5$  is a

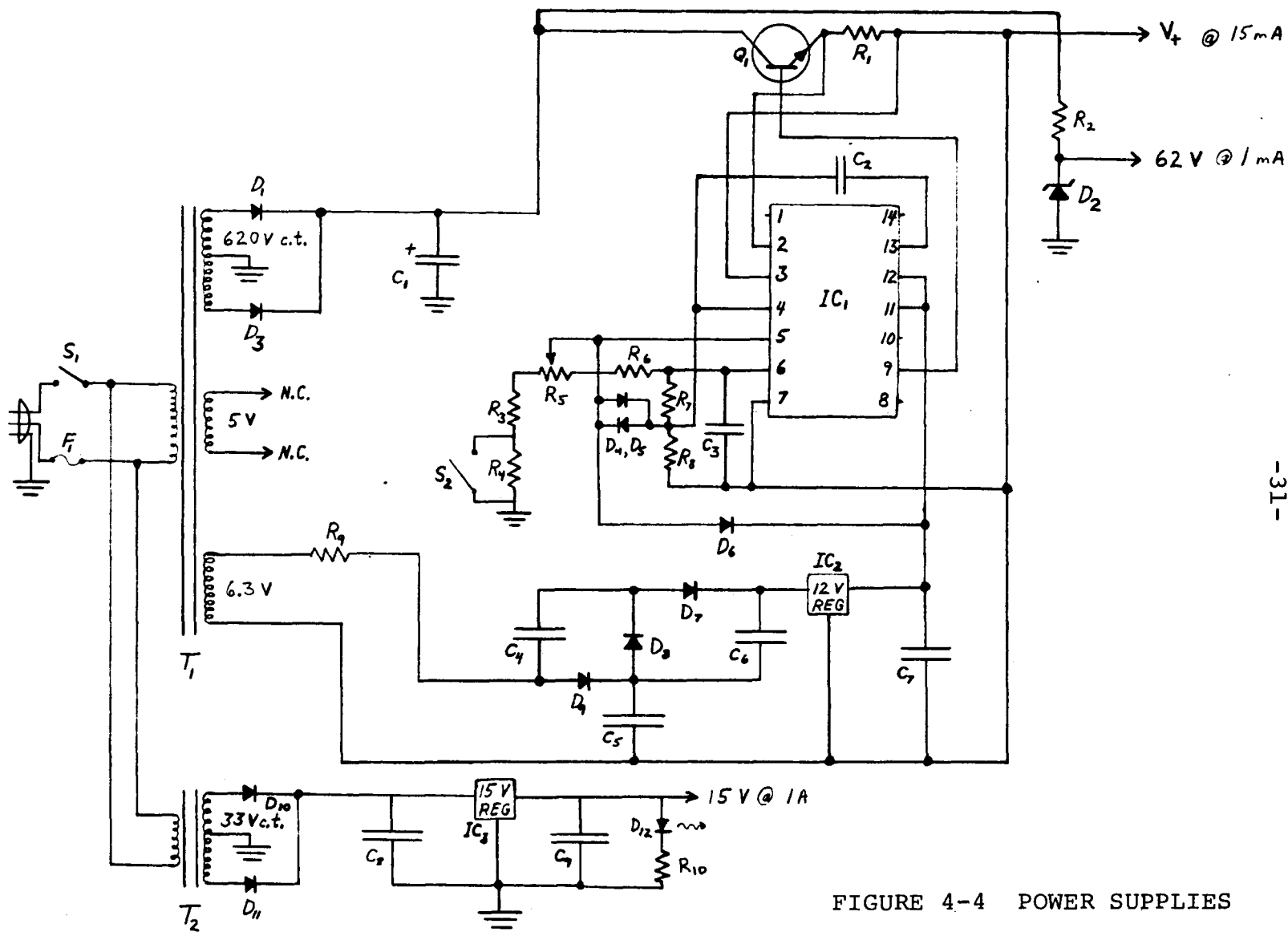


FIGURE 4-4 POWER SUPPLIES

ten turn potentiometer which controls the high voltage and  $S_2$  is the range switch.  $D_4 - D_6$  and  $C_3$  are for protection purposes. Since the zero of the 12V regulator supply needs to be at the output voltage level  $V_+$ , a floating 12V regulator supply was also needed. To obtain this, the 6.3V filament winding of the transformer was tripled and regulated to power IC1. Measured regulation of the circuit is  $\pm 0.01\%$ . A conventional 15V supply was also included to power low voltage circuits like the pulse generator and digital panel meter.

#### 4.5 Digital Panel Meter

To read the high voltage value, a digital panel meter was incorporated in the control unit (fig 4-5). To read the voltage to the nearest tenth of a volt up to 400.0 volts, four digit capability is needed. An Intersil 4 1/2 digit system was chosen because of its relatively low cost, low parts count, and versatility. Although the version constructed used LED displays, a pin for pin compatible LCD driver also exists. The digital system has capability to a full 4 1/2 digits and auto zero. Since the control unit already contained a + 15V supply, a 5V regulator was used to supply the digital circuits, and a 555 timer was used to provide both a clock signal and a (nominal) - 15V supply. Meter accuracy is  $\pm 1$  digit, although instabilities in the 555 clock circuit produced some digit rollover. A more stable clock would be preferable.



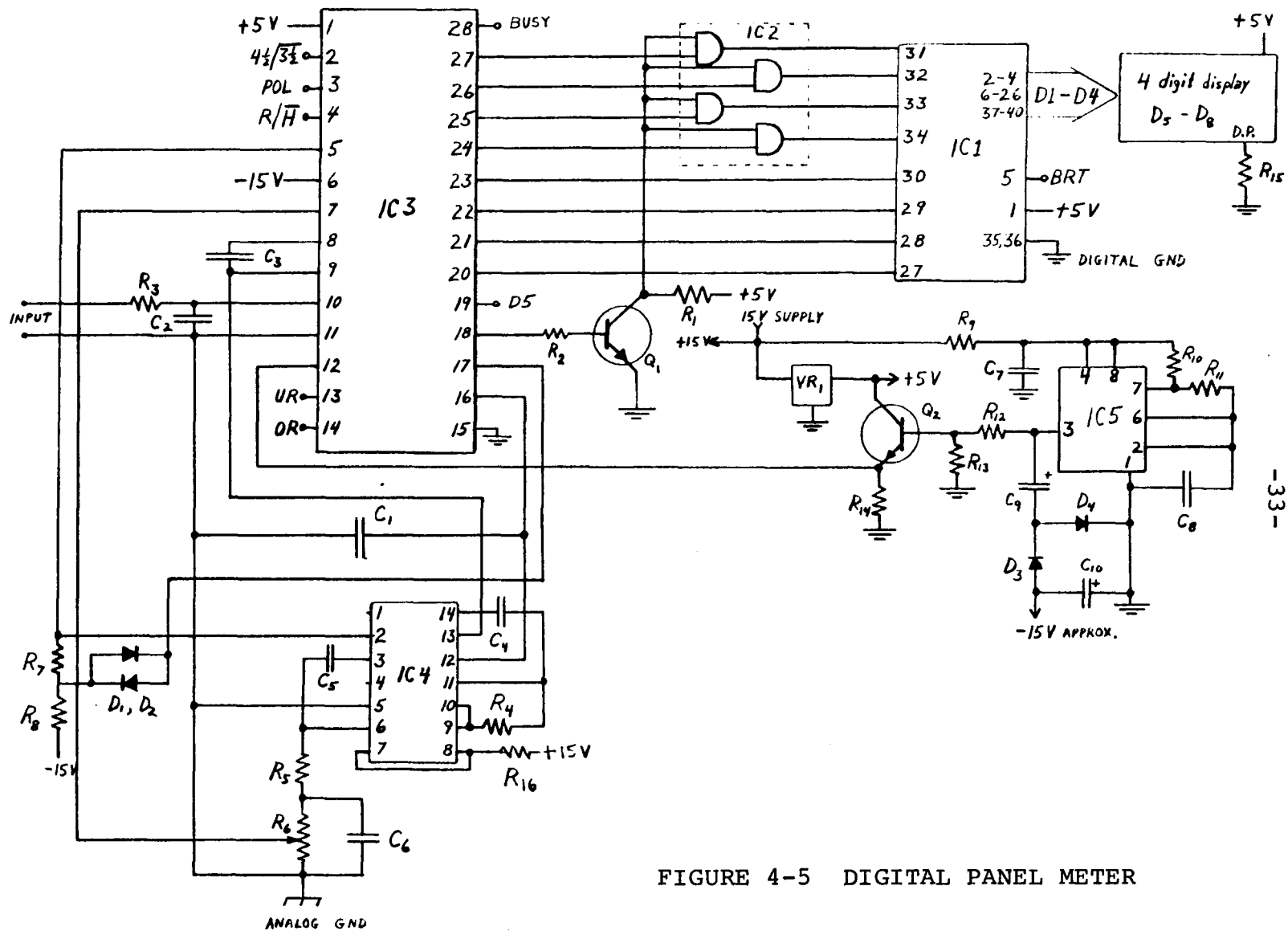


FIGURE 4-5 DIGITAL PANEL METER

## 5. LASER HEAD CHARACTERISTICS

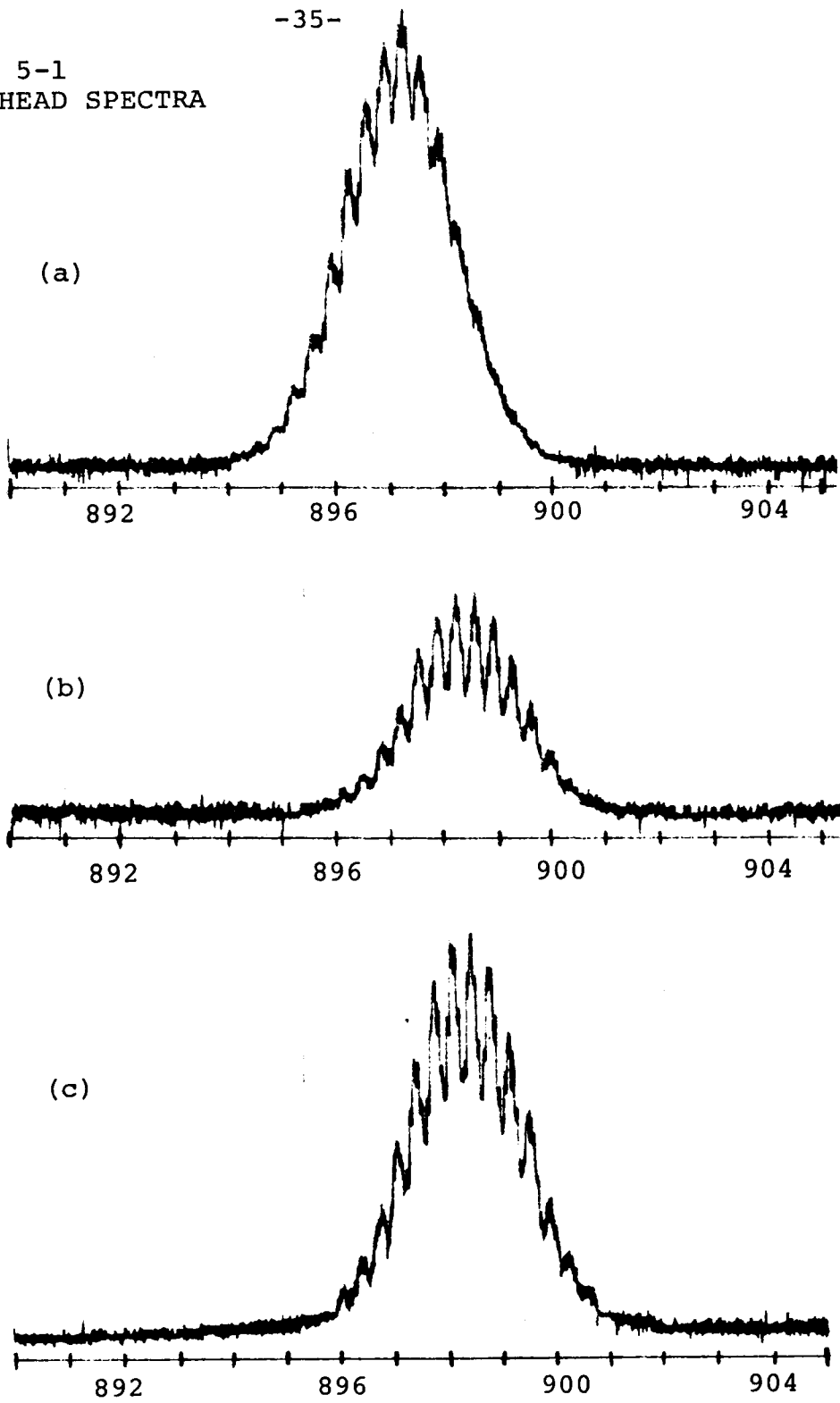
Most of the experimental work was done using the first laser head constructed. This design was already under development when I arrived at Opto-Electronics Limited, and I constructed the laser head and optimized circuit parameters. The laser head output consisted of a fast primary light pulse and a much smaller second pulse. The first pulse had a minimum width of 60-70 psec with a supply voltage of 230V, estimated by deconvoluting the response observed with a fast detector. The second pulse occurred approximately 200 psec after the first, and had an amplitude about 7% of the first.

Time averaged spectra were taken of this source and are shown in figures 5-1(a) to 5-1(c). Fig. 5-1(a) shows the spectrum with  $V_+ = 242V$  to the laser head. This was done first since the light output was higher with the higher pumping current. Fig. 5-1(b) shows the spectrum at  $V_+ = 230V$  on the same vertical scale. This was the setting for minimum pulse width. Fig. 5-1(c) shows the same scan on an expanded vertical scale. The central wavelength and the spectral width were  $898.4 \pm 0.1nm$  and  $2.4 \pm 0.1nm$  respectively for  $V_+ = 230V$  and  $897.3 \pm 0.1nm$  and  $2.4 \pm 0.1nm$  for  $V_+ = 242V$ .

A second laser head was constructed which gave a 900psec pulse for the OTDR setup. A different drive transistor was used in the laser head, which had a slower risetime and lower voltage capability. The laser head was run at  $V_+ = 180V$  and the optical output was much lower than the other head.

-35-

FIGURE 5-1  
LASER HEAD SPECTRA



## 6. OTDR EXPERIMENTS

### 6.1 Optical Y Couplers

The tapered biconical coupler was chosen for use in these experiments mainly because of its low cost and availability of components. It was also originally thought that construction would be fairly simple, however the practical construction of these couplers is more difficult than it would at first appear. The fibers are much more fragile after they have been heated and tapered. They also become soft at a temperature which is much lower than their melting temperature. Thus at first problems were caused by the fibers tapering or expanding and moving before they were fused together. At first the fibers were pulled by hand, but the best results were obtained when a jig which provided a very light spring pressure was used to pull the coupler as it was being heated.

The measured coupling efficiency was highly dependent on the measurement method due to various modes being excited and different numerical apertures for fibers and sources or detectors. For a fiber Y coupler, McMahon<sup>10</sup> states that the most efficient coupling possible for equal sized fibers is 50% coupled in, 50% coupled out on return (fig. 6-1(a), 6-1(b)). Although other methods gave higher coupling efficiency, the most realistic setup for coupler loss measurements was decided to be fig. 6-2(a), 6-2(b). Since the light from the source will be coupled into the test fiber and travel a relatively long distance

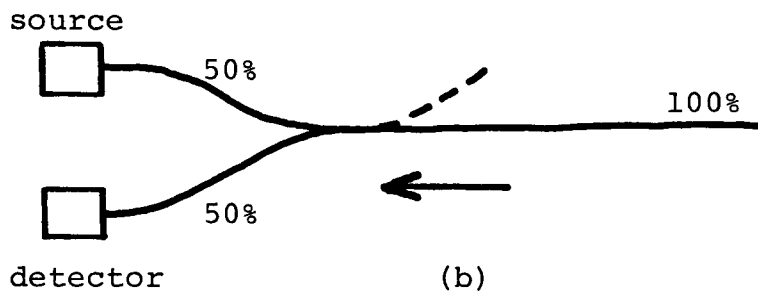
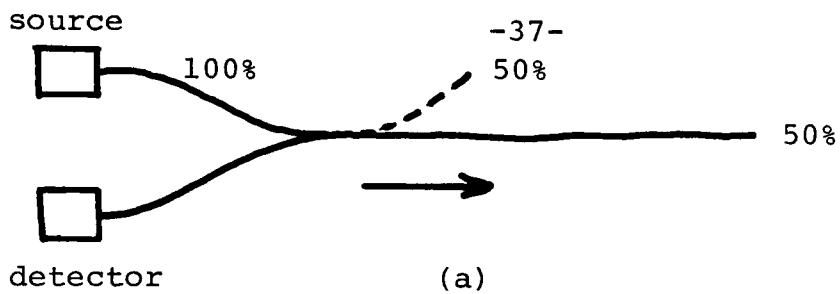


Figure 6-1 Lossless Coupling Efficiency

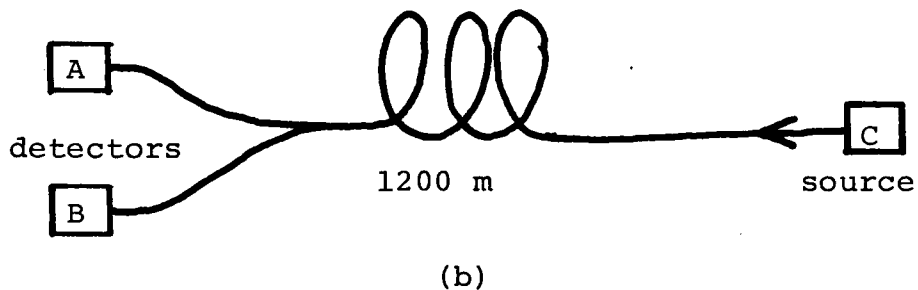
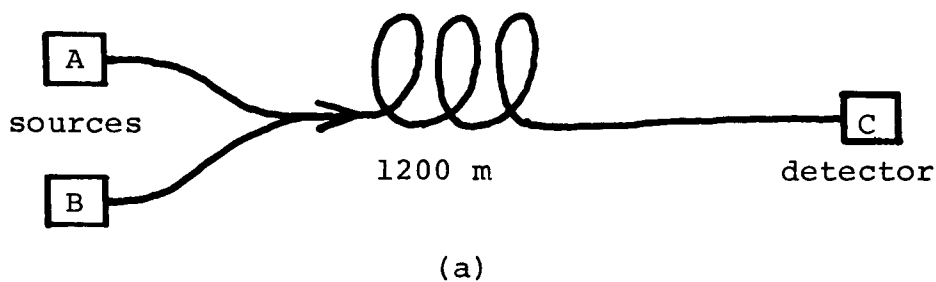


Figure 6-2 Measuring Actual Coupling Efficiency

before reflection, the coupler efficiency in that direction was measured with a 1200m length of fiber butted to the coupler. In the other direction, the signal travels down the fiber before it reaches the coupler, and then goes straight into the detector. Thus the setup in Fig 6-2(b) was used. For the first setup, using end A to launch the signal, 13% of the light reached end C. (The reference 100% signal was obtained with a short fiber butted to the 1200m length.) With end B as the source, 1.8% of the light reached end C. For the second setup with C as the source, 16% reached the detector in position A and 3.1% reached the detector in position B. The higher efficiency in the second case is expected since the coupler excites lossy higher order and cladding modes<sup>1</sup>. This light will be lost in the 1200m fiber in the first case, while the short distance to the detector in the second case allows it to be captured. Thus the most efficient system was A as the source, B as the detector, giving an overall efficiency of 0.40%, compared to the theoretical coupling efficiency of 25%, an excess optical loss of 18 dB. This loss figure could not be improved using the construction methods employed, although other workers have reported much lower losses<sup>9</sup>.

## 6.2 Experimental Setup

The OTDR experiments were done with the setup in Fig. 6-3, using the coupler characterized earlier. Since the coupler was so lossy, the return signal was small, even for the most favourable case of a good cleave, when 4% of the test signal was returned.

The original detector-source combination used was the 70 psec source with the gain of 50 avalanche detector to give a combined FWHM of

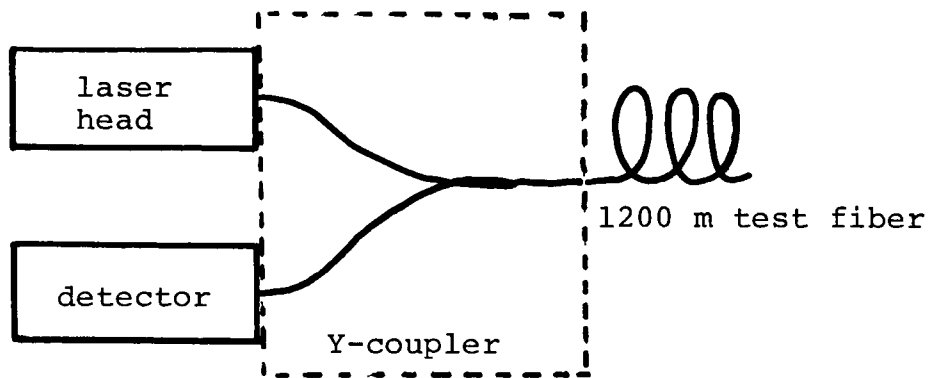


Figure 6-3 Experimental OTDR Setup

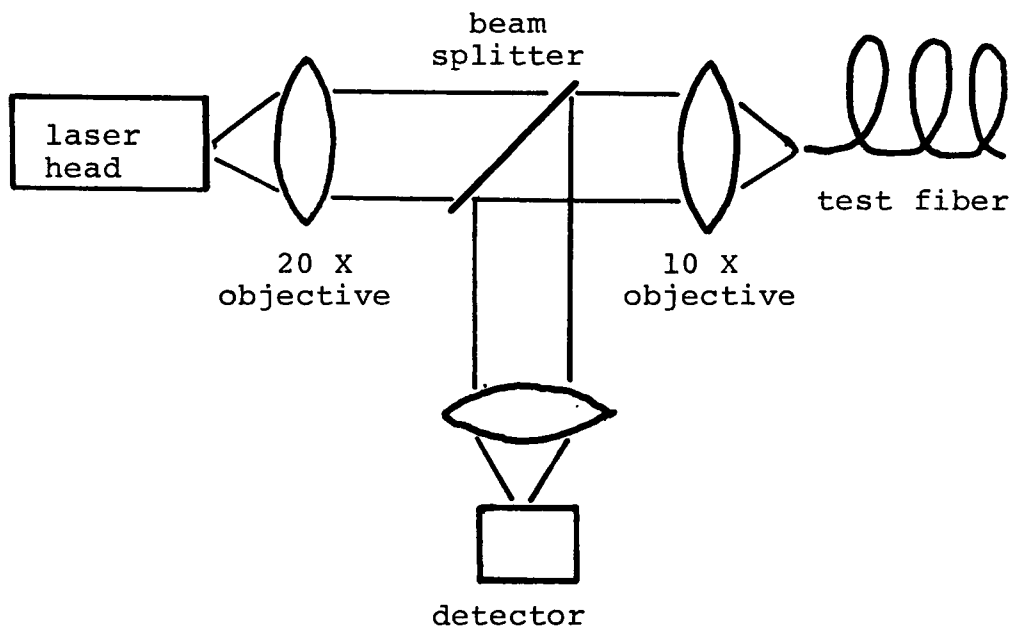


Figure 6-4 Reflection Coefficient Measurements

140 psec. The fiber used for testing the system was a 1200m length of 300 MHz-km fiber. This bandwidth broadened the return pulse to approximately 4 nsec. Since the pulse width increased, the pulse height decreased by approximately the same ratio. Thus the relative signal amplitude decreased to  $0.24/4 = 0.035$  or 3.5% and the observed return signal was  $2 \pm 0.5$  mV. Substituting the appropriate values ( $S = 0.2$  A/W,  $G = 50$ ,  $R_L = 50\Omega$ ,  $P_O = 2$  W,  $T_\ell = 0.5$ ,  $T_d = 0.5$  with 18dB excess loss,  $n = 0.04$ ,  $\alpha = 3.5$  dB/km,  $L = 1.2$  km,  $D = 0.035$ ) into equation 3 gives a detected voltage  $V_d = 1$ mV. The discrepancy between this value and the experimental value is probably due to underestimating the laser power and/or the avalanche detector gain.

The second laser source was built to have a wider pulse and not be as affected by dispersion. However, as stated earlier, the peak light output from this laser head was much smaller than the original. Thus while the signal did not decrease in amplitude as much due to dispersion, it started at a lower level and thus was no improvement, ~1mV return signal with the 300 gain detector.

Since the return signal was so small, an extra mirror was butted to the fiber end to give a larger return and enable a measurement of 4-5 nsec for the round trip dispersion. The dispersion was also checked in the transmission mode, and found to be 2.2 nsec. Since the material dispersion is typically an order of magnitude smaller (<200 psec/km), virtually all the measured dispersion was due to modal dispersion.

### 6.3 Single Mode Fibers

The experimental setup above was not used to test single mode



fibers since the signal level was already low and the coupling ratio between two fibers goes as their core areas. The coupler core was  $62\text{ }\mu\text{m}$  in diameter, while the single mode fiber core was  $2\text{ }\mu\text{m}$  in diameter. Both had numerical apertures of 0.20. However, a straight length of single mode fiber was tried to check signal levels, and it seemed to cause no problems. Signal levels were ~10% of those obtained with the graded index fibers, although some of the signal may have been from cladding modes (the fiber was 1m long). Various designs have been produced for single mode fiber couplers, and it appears there would be little difficulty in carrying the OTDR design over to single mode fibers. Since the pulse dispersion would be much smaller, a faster pulse source and detector would be useable, enabling measurements to (equation (5))  $22\text{ GHz-km}$ .

#### 6.4 Reflection Coefficients for Non-Ideal Breaks

Since one use of a practical OTDR system would be checking for breaks in an optical fiber, experiments were done to measure the reflection coefficients of non-ideal (i.e. non-cleaved) fiber breaks. A lens-beam splitter arrangement was used (fig. 6-4) because of the low signal levels involved. This resulted in a signal approximately 8 times larger than with the Y-coupler.

The first type of break which was investigated was the breaking of the fiber due to being forced to form too small a diameter circle. The fiber was held in a loop and slowly pulled until it broke. With the 4% reflection from a perfect cleave as a reference, this method of breaking yielded an average reflection coefficient of 0.64% with a

standard deviation of  $\pm 0.16\%$ .

The next method attempted was breakage due to tension, but the fibers were very difficult to grip or clamp without scratching the fiber and forming a flaw. This it was not possible to break the fiber solely due to the tension applied.

Melting the fiber was also tried. The fiber was held with a slight tension applied and heated until it melted in two. The reflection coefficient here was slightly higher at  $0.85\% \pm 0.3\%$ .

The last measurements taken were for crushed fiber. The fiber was crushed against a metal surface by a screwdriver blade. This yielded the lowest average reflection coefficient,  $0.2\% \pm 0.2\%$ . Even with this method, however, the lowest reflection coefficient from the non-ideal break was  $\sim 0.1\%$ , only 40X or 16dB below the coefficient for a perfect cleave. Thus for the proposed systems with good Y couplers (1-2 dB loss as opposed to 18dB loss) there would be no difficulty in detecting any of these types of breaks.

## 7 OTDR SYSTEM RECOMMENDATIONS

### 7.1 Couplers

The various methods used to fabricate the biconical taper couplers did not produce any satisfactory Y couplers. As reported, the best excess optical loss was 18 dB. Commercial couplers of various constructions (chapter 3) are available with excess losses of 1 - 2 dB and thus it is clear that a great improvement in signal is possible by either making or purchasing a better coupler. From the experience with the fused biconical taper coupler, it would not seem to be a good choice for production use. There would still be a lot of research to be done just to produce a good coupler, and then it would appear to be difficult to mass produce. It seems that the Selfoc couplers (fig. 3-7) would be the easiest to construct reproducibly, with the evaporated beamsplitter film and mechanical alignment being the most difficult parts of construction. Neither of these should pose any major problems. It should also be possible to make this type of coupler for use with single mode fibers.

### 7.2 Pulse Width

From the measurements taken, it is clear that the pulse width will have to be tailored for the type of fiber being tested. For 1 km of 300 - 1000 MHz-km graded index fibers, the 150 psec source - detector pulse was excessively short, and didn't provide any more information than a 1 nsec pulse, while yielding a small signal due to dispersion.

Thus for these graded index fibers, a pulse width of approximately 1 nsec is needed for a practical instrument. This still enables measurement of pulse dispersion over 500m, while giving a large enough return signal for a 4 - 5 km measurement range.

For single mode fibers, a short pulse is a must, especially if the wavelength is  $\sim 1300\text{nm}$ . Here dispersion is not nearly as high, and a short pulse is needed to give good estimates of the fiber bandwidth. One problem which will arise with this system is getting long time, low jitter trigger delays. One possibility is a fixed length of fiber with a separate source and detector to produce a delayed trigger signal.

### 7.3 Amplifiers

Another possibility for increasing the return signal amplitude is the use of a high speed amplifier. Economical (\$25-50) wideband cascable amplifiers are available with bandwidths up to  $\sim 1\text{ GHz}$ <sup>12</sup>. This is not high enough for use with the single mode fiber pulses, but it is high enough to use with the 1 nsec pulses. These amplifiers each have gains of 9-13 dB, and are easily cascable. The maximum power output in this series is +15 dBm, corresponding to  $\pm 1.7$  volts peak output. Typical specifications for three of these amplifiers, as well as a cascade of the three, are shown in table 3. These amplifiers have low enough noise figures that the avalanche shot noise and the amplifier equivalent input noise are of the same order of magnitude, and either would only be visible on the oscilloscope for gains  $> 30\text{ dB}$ .

Table 3

Avantek	GPD 461	GPD 462	GPD 464	Cascade
High Frequency Limit (-3dB)	>900 Mhz	>1000 MHz	>1000 MHz	>800 MHz
Low Frequency Limit (-3dB)	- - -set by external capacitors - - - -			
Gain (dB minimum)	13	13	9	35
Noise Figure	4.5	6.0	7.5	4.9
Power Output (1dB gain comp.)	-2dBm	+6dBm	+15dBm	+15dBm
Output Pulse Width, 1 nsec pulse in	1.14	1.11	1.11	1.32

## 8 CONCLUSIONS

Two different OTDR instruments are necessary for the two types of fiber which will be in common use in the future. For single mode fibers, the shortest light pulse possible is necessary to give useable measurements. The test wavelength should also be the same as the wavelength of the link laser, presumably around 1300 nm. Finally, because of the large difference in sizes between the single mode and multimode fibers, the Y coupler would have to be designed specifically for the single mode fiber. If backscattering attenuation measurements were desired, a longer pulse would be necessary.

For multimode, graded index fibers, the optimum pulse width seems to be approximately 1 nsec. With this width, the dispersion can be measured for lengths  $\geq 500$  m, but it does not decrease the signal amplitude excessively. Inexpensive pulsed lasers at 800-900 nm can be used for the source, and there are reasonably simple couplers available.

For the system which was set up for this project, a satisfactory Y coupler would increase the optical signal by at least 15 dB or 30X. A 1 nsec light pulse of comparable intensity to the 70 psec pulse would effectively give another 10X or 10 dB more light for a 1 km graded index fiber. Thus this system would be able to detect signals 25 dB below the 4% reflection, with a dynamic range limited only by the avalanche detector. As stated in section 6.4, the lowest measured reflection coefficient was 16 dB below the 4% reflection, and thus this instrument

would be able to detect and locate all the experimental breaks for 1 km of fibre.

The Rayleigh scattering level for a 1 nsec pulse will be typically 50 dB below the 4% reflection. To detect this level of signal, amplification would be necessary. 30 dB of amplification would enable detection of signals 55 dB below a perfect break. Here the dynamic range would be limited by the amplifiers to 58 dB before gain compression took place. Thus Rayleigh scattering signals and fibre losses could readily be measured using avalanche detectors and 30 db gain amplifiers.

#### REFERENCES

1. Y. Ueno and M. Shimizu, "Optical Fiber Fault Location Method", Appl. Opt. 15, 1385 (1976).
2. S.D. Personick, "Photon Probe - An Optical Fiber Time Domain Reflectometer", Bell Syst. Tech. J. 56, 355 (1977).
3. M.K. Barnoski and S.M. Jensen, "Fiber Waveguides - A Novel Technique for Investigating Attenuation Characteristics", Appl. Opt. 15, 2112 (1976).
4. E.-G. Neumann, "Optical Time Domain Reflectometer: Comment", Appl. Opt. 17, 1675 (1978).
5. S.E. Miller and A.G. Chynoweth, eds., "Optical Fiber Telecommunications", Academic Press, N.Y., 1979.
6. F.P. Kapron, "Maximum Information Capacity of Fiber-Optic Waveguides", Electron. Lett. 13, 96 (1977).
7. D.N. Payne and A.H. Hartog, "Determination of the Wavelength of Zero Material Dispersion in Optical Fibers by Pulse Delay Measurements", Electron. Lett. 13, 627 (1977).
8. W.J. Tomlinson, "Applications of GRIN-rod Lenses in Optical Fiber Communication Systems", Appl. Opt. 19, 1127 (1980).
9. G.S. Duck, "Fiber Optic Telephone System Optical Components", Masters Project, McMaster University, 1979.
10. D.H. McMahon, "Efficiency Limitations Imposed by Thermodynamics on Optical Coupling in Fiber Optic Data Links", J. Opt. Soc. Am. 65, 1479 (1975).
11. B.S. Kawasaki and K.O. Hill, "Low Loss Access Coupler for Multimode Optical Fiber Distribution Networks", Appl. Opt. 16, 1794 (1977).
12. AvanteK, "Design with GPD Amplifiers, 3rd. ed.", Santa Clara, California, 1980.